

Bistatic RCS Control on Slot-Sinuuous Antenna by Adding 3 and 5 Parasitic Ellipses Openings

Elson Agastra*, Alaksander Biberaj, Olimpjon Shurdi, and Bexhet Kamo

Abstract—In this paper, an ultra-wide band modified slot-sinuuous antenna has been designed to enhance bistatic radar cross section (RCS) response. The design procedure consists of adding three or five parasitic ellipses openings to each of the slot-sinuuous arm cells. The parasitic ellipsis allows to control bistatic RCS without impacting antenna radiation characteristics. Parasitic ellipses opening dimensions are small compared to the relative wavelength of the signal on each active region of the antenna. The ellipses distributed on sinuous antenna arm are scaled by the same expansion coefficient used to design the antenna itself. In the proposed design, ellipses parameters such as ellipses axis, radial position, and relative angle position on the sinuous cell are key parameters to be optimized for bistatic RCS reduction. The total number of designing parameters is finite, but their combination is infinite, which leads to the possibility of designing different antennas based on the required designing goals. The proposed solution and the results presented in this work show the applicability of the designing parameters to control bistatic RCS on active region antennas.

1. INTRODUCTION

The demand of military applications for object tracking and recognition has always been a very powerful engine in research and development on radar and microwave imaging applications [1–4]. The demand on high performance radar systems requirement goes parallel to the objective of the radar itself as invisible as possible to hostile radars. This last requirement means radar systems with the lowest possible equivalent radar cross section (RCS).

One of the key elements for designing high performance radar systems with the lowest radar cross section is the antenna itself which is an exposed radar element to possible hostile radars.

In recent years, various techniques have been designed to reduce or control antenna radar cross section in a monostatic or bistatic scenarios. First attempts reduc RCS are based on using antenna shaping as to reflects incident waves on directions that differ from the incident one. This was one of the first stealth techniques used to reduce object monostatic RCS [1, 5]. This solution improves the stealth response of the object on monostatic radars but is less effective on bistatic radar solutions [5, 6]. Another technique used to reduce radar footprint of the object is using radio absorbing materials which have drawback in increasing the overall antenna dimensions and can potentially reduce antenna performance [7].

Many different approaches have been presented for RCS reductions such as frequency selective surfaces (FSS) [8–10], metasurfaces [11–14], partially reflecting surfaces [15], electromagnetic bang gap (EBG) structures [16], and artificial magnetic conductor [17, 18]. Different authors have presented parasitic stubs or slots openings in the antenna structure or in the antenna ground plane to control in band RCS [19–23]. Slots openings vary from standard geometries such as rectangular or square slots, circular, star, up to any fractal geometries or combinations of elementary ones [19, 24, 25].

Received 14 July 2022, Accepted 25 August 2022, Scheduled 9 September 2022

* Corresponding author: Elson Agastra (eagastra@fti.edu.al).

The authors are with Department of Electronic and Telecommunications, Polytechnic University of Tirana, Tirana, Albania.

Reducing radar cross section is not an easy task specially on ultra-wide band (UWB) radar systems where most of the techniques mentioned above present narrow band response or are focused on out-of-band RCS reduction.

In this work, a slot-sinuous antenna, designed to operate in 6–18 GHz frequency band, is modified by adding parasitic ellipses slots. The proposed antenna is used in radar applications due to its intrinsic wide-band characteristics [1, 26–28]. The design is based on the slot-sinuous presented in [19, 29]. Ellipse slot openings are rated suitable for RCS in-band reduction similar to what is presented by the authors in [19] and by other authors on broadband antennas [22, 24, 30–32], antenna arrays [33], etc.

The paper is organized as follows. In Section 2, the antenna design parameters are drafted and geometrically explained. Section 3 defines simulation parameters and metrics used to evaluate the proposed solution such as radar cross section and the difference on bistatic radar cross section between the two analyzed antenna models. Section 4 addresses bistatic radar cross section reduction using the proposed solution. In this section, some important remarks are added to help the reader better understand the physical meaning of the proposed solution and how this solution can be applied in similar projects. At the end, in Section 5, some concluding remarks are drawn for the presented work.

2. ANTENNA DESIGN DEFINITION

Sinuous antenna has been recently chosen as radar system radiating element due to its intrinsic UWB characteristics [1, 27, 28].

Sinuous antenna is categorized as active region antenna and is designed based on a quasi-periodic geometry defined in cells as in Figure 1 [29]. In each frequency, in the designed frequency band, we can find a physical antenna area where the current distribution has a major contribution to the radiation characteristics.

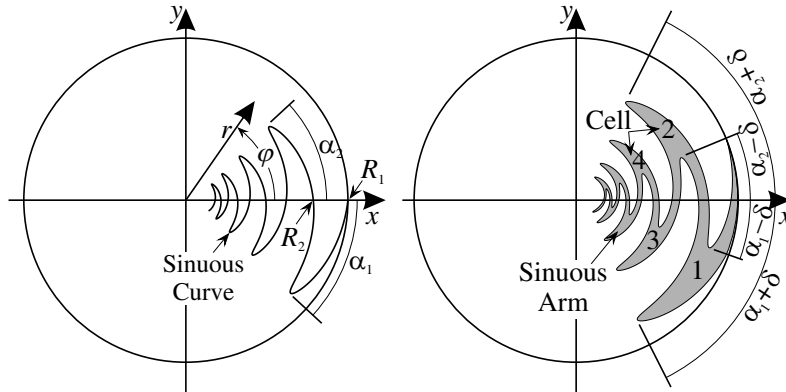


Figure 1. Sinuous antenna design geometry.

Sinuous geometry can be designed based on mathematical formulation defined in (1).

$$\varphi = (-1)^p \alpha_p \sin \left[\frac{\pi \ln(r/R_p)}{\ln(\tau_p)} \right] \quad (1)$$

where r and φ are polar coordinates of the points describing sinuous curve relative to the p th antenna cell. Cell no. 1 is the outermost cell, with radius R_1 . The following cells are designed based on a logarithmic recursive rule, $R_p = \tau_{p-1} \times R_{p-1}$, where τ_p and α are appropriate constants describing angular width and scale factor of the antenna, like log-periodic antenna design.

The boundaries of sinuous antenna arm are designed by rotating the obtained curve as in analytic expression (1), by $\pm\delta$ around the z axis.

In the present design, the chosen parameters allow a complementary antenna design, which means that the metallic and non-metallic areas are identical in four arm version. To obtain a self-complementary structure, designing antenna parameters are: $\tau_p = \tau = 0.77$, $\alpha_p = \alpha = 45^\circ$ and $\delta_p = \delta = 22.5^\circ$ and 11 total cells ($P = 11$).

Sinuuous antenna, in its four arm version, allows contemporary two orthogonal polarizations that can be two orthogonal linear polarizations VP and HP (*VP*-Vertical Polarization and *HP*-Horizontal Polarization) or two orthogonal circular polarizations RHCP and LHCP (*RHCP*-Right Hand Circular Polarization and *LHCP*-Left Hand Circular Polarization) as presented in Figure 2. This sinuuous antenna feature with its intrinsic ultra-wide bandwidth behaviour makes the sinuuous antenna a very interesting element for radar systems.

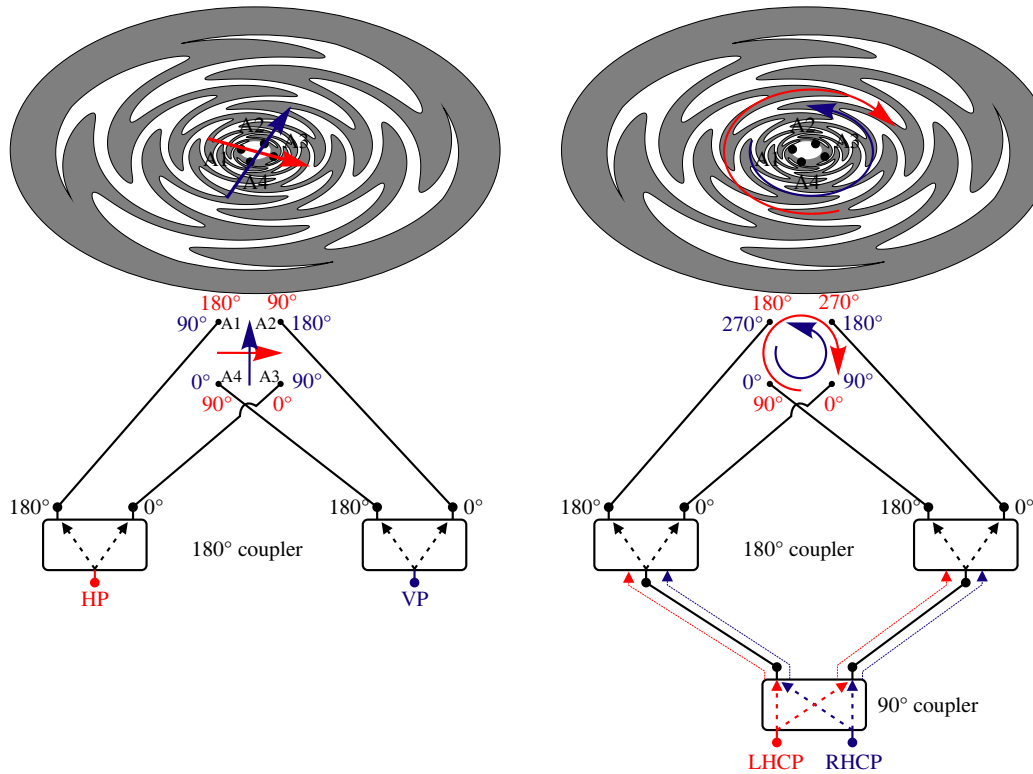


Figure 2. Geometry of parasitic ellipsis slots openings to the metallic surface.

In this work, a four arm slot-sinuuous antenna is investigated for right hand circular polarization and its cross-polar, left hand circular polarization. For the chosen frequency band (6–18 GHz), the maximum sinuuous arm radius is 14 mm, and the overall antenna radius, including the closing rings needed to realize the slot-sinuuous antenna, is 18 mm [29].

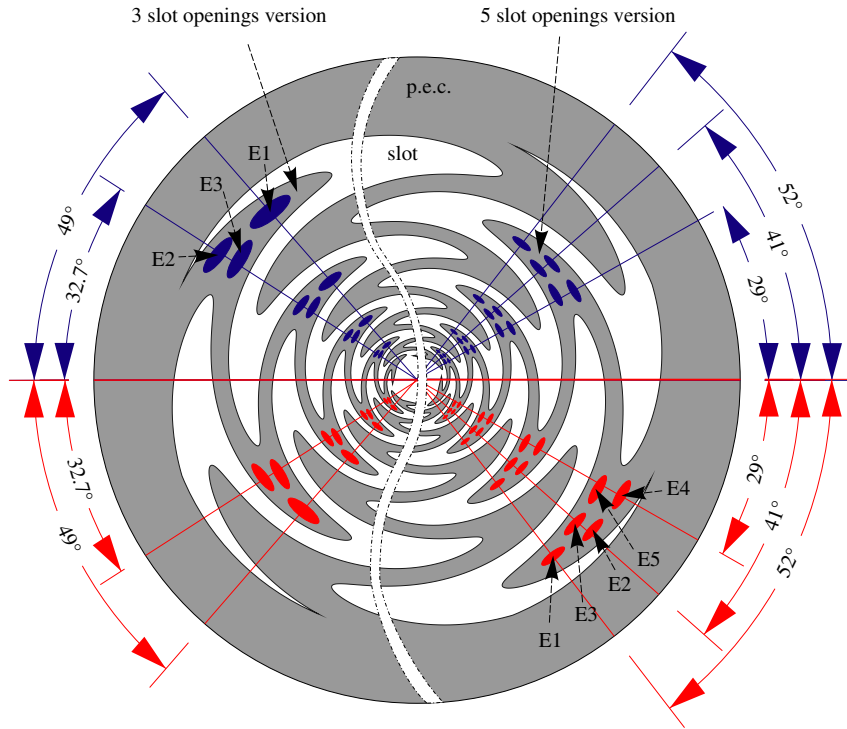
The aim of this work is to add small parasitic ellipsis openings to the antenna structure to control bistatic radar cross section continuing authors previous work [19] on monostatic radar cross section. The above term of “small parasitic” ellipses are relative to signal wavelength on the active region of the antenna where the ellipses are deployed. In this way, the parasitic openings have a minor impact on the radiation characteristics of the antenna itself.

In this work, starting from the standard slot-sinuuous antenna [29], two antenna versions are investigated for RCS modification, the first one with three ellipses openings on each arm cell (3S) and the second version with five ellipses openings (5S) [19]. For the chosen design, ellipsis positioning on each sinuuous arm cell, for both models, is presented in Figure 3, and relative designing parameters are defined in Table 1. Each ellipse dimension is chosen as to have low disturbance to the electrical current flow in the sinuuous antenna arm. As will be more clear in Section 4, ellipses dimensions and their positions are not a trivial solution.

Details of ellipses designing parameters and positioning are presented in Figure 4. In this project, we have chosen to design all ellipses (3 or 5 per sinuuous cell) tangent to the same sinuuous curve that defines the center of the outermost ellipse (*E1*), as in Figure 4. This condition is not necessary, and the arrangement of the ellipses can be any inside the cell, but in our simulation this choice has produced

Table 1. Ellipses dimensions on the outermost cell for both antennas models.

Ellipses	3 slots model		5 slots model	
	Major axis (mm)	Axial ratio	Major axis (mm)	Axial ratio
$E1$	0.30	4	0.30	3
$E2$	0.33	4	0.30	3
$E3$	0.28	4	0.27	3
$E4$	-	-	0.28	3
$E5$	-	-	0.26	3

**Figure 3.** Geometry of parasitic ellipsis slots openings to the metallic surface.

better results.

Ellipse $E1$ is positioned at the edge of the sinuous curve, at an angle of 49° for three slot version (equivalent of $\delta_{E1} = 5^\circ$ relative to Figure 1), with its major axis perpendicular to the respective radius (R_1) from the antenna center. $E2$ and $E3$ ellipses major axis is positioned tangent to the same sinuous curve used to define the center of ellipses $E1$. In this case, their respective centers are moved $\pm 1.5^\circ$ from the defined 32.7° angular direction. What we have presented in Figure 4 is actually the best trade-off we obtained in our simulations for three ellipses openings as will be clearer in Section 4. More in general, these are designing parameters that can be changed to modify the RCS response of the entire structure. The mentioned parameters are designing degree of freedom of the RCS control, constrained to each other, and the available physical space in the sinuous cell.

In the present project design, we have to define five parameters:

- N : Total number of ellipses in each sinuous cell, (i.e., 3, 5, 7, etc. odd number);
- A_{\max} : Ellipsis major axis dimension;
- A_R : Ellipsis axial ratio;

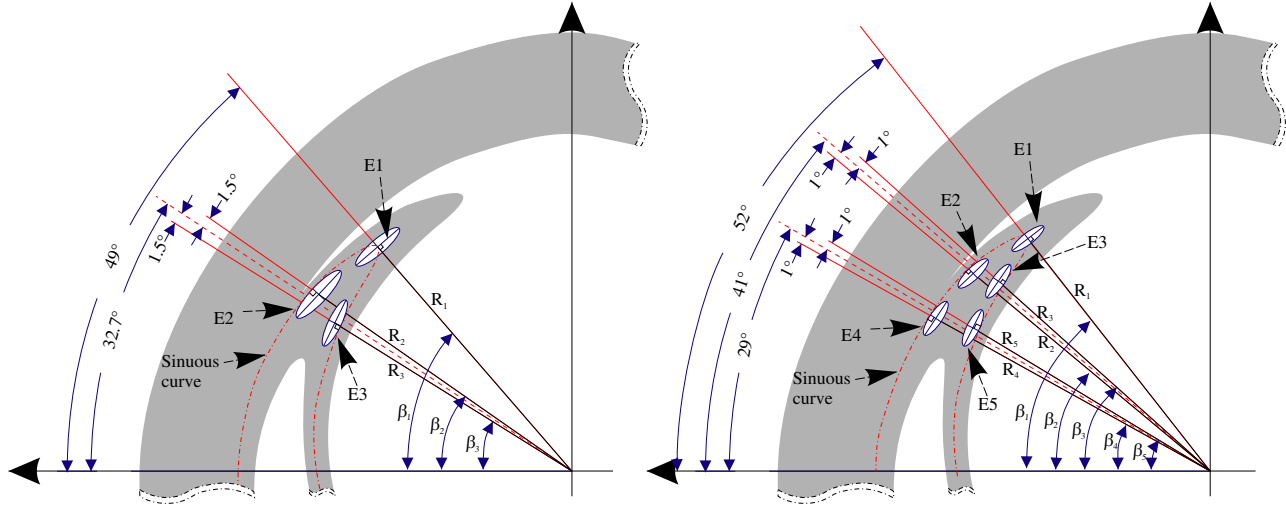


Figure 4. Ellipses slot openings definition parameters.

- R : Ellipses radial position from antenna center;
- β : Ellipses angular position.

In this definition, we have assumed that the ellipses are tangent to a sinuous curve ($E2$, $E3$, $E4$, $E5$, etc.), and only the first ellipse is orthogonal to the position radius from the antenna center ($E1$). In the more general case, we need to introduce a new variable for the orientation of the ellipses inside the sinuous cell. In this project, we have not investigated other ellipses orientations.

All five designing parameters are correlated to each other, as the ellipses cannot overlap to each other and cannot cross the sinuous arm which will disturb the equivalent of magnetic current.

In both designs, ellipses axis and their radial position on each sinuous cell are scaled by the same τ factor used in the sinuous curve design as above ($\tau = 0.77$). This permits to have the same behavior over the entire frequency band, like the antenna itself.

Both antennas are designed and investigated using ANSYS HFSS [34], V.15. The CAD models of the antennas are shown in Figure 5 where absorbing radiofrequency material is added in the half lower space to suppress back radiating as part of the original antenna design.

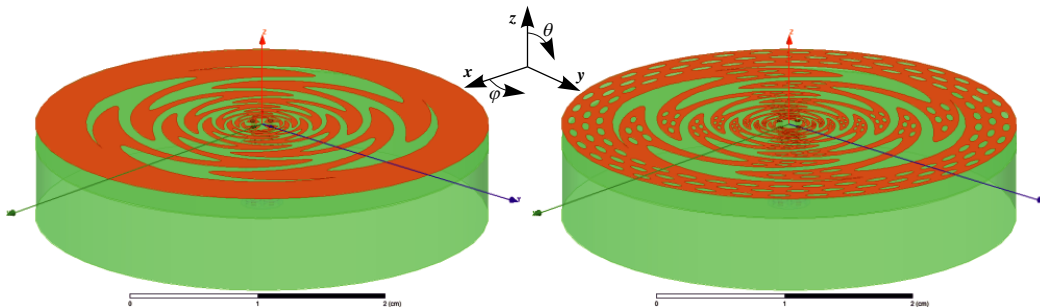


Figure 5. CAD models on HFSS of standard slot-sinuous and modified one.

3. SIMULATION PARAMETERS AND PERFORMANCE ANALYSIS

Antenna radar cross section is formed by the contribution of two factors: structural mode RCS and antenna mode RCS [33, 35] and mathematically defined in Equation (2).

$$\sigma = \left| \sqrt{\sigma_s} - (1 - \Gamma_a) \sqrt{\sigma_a} e^{j\phi} \right|^2 \tag{2}$$

where σ is the total antenna RCS, and σ_s and σ_a are, respectively, structural and antenna RCSs. The first is related to the antenna structure as seen from incident electromagnetic field with antenna terminals shorted circuit, and the second one also evaluates the antenna impedance match at the feeding port. Both are related by the phase difference ϕ and by the reflection coefficient at feeding port Γ_a . The reader must pay attention to the definition of the reflection coefficient (Γ), which, as normally seen from the generator toward the shorted-circuited antenna terminals, is $\Gamma = -1$ as in Equation (3a) [35]. But for antenna seen as scattering element and the RCS defined in Equation (2), the definition of Γ_a is from the shorted terminals toward the antenna itself, which for the shorted-circuit terminals ($Z_L = 0$) gives $\Gamma_a = 1$ as in Equation (3b) [35]. A more detailed description of the definition of antenna scattering can be found in [35]. From the definition of reflection coefficient as in Equation (3b) and shorted circuit of antenna terminals, this results in $\sigma = \sigma_s$ from Equation (2).

$$\underbrace{\Gamma = \frac{Z_L - Z_0}{Z_L + Z_0}}_{(a)} \quad \underbrace{\Gamma_a = \frac{Z_a - Z_L}{Z_a + Z_L}}_{(b)} \quad (3)$$

In this material, only the equivalent structural RCS has been investigated for both antennas as to better understand the influence of parasitic slots openings to the structural RCS.

As to better evaluate the design parameters choice on the structural radar cross section and to compare the obtained results, in this material, a difference on RCS between the two antenna models is used as defined in Equation (4).

$$\Delta\sigma = \sigma_{3Slot} - \sigma_{5Slot} \quad (4)$$

Due to the designed antenna overall area, RCS on both antenna models will be smaller than 0 dBsm. Applying Equation (4), if positive values are found, it means that the obtained RCS for 5 slot model is better (smaller values) than that on 3 slot model, and vice-versa.

4. NUMERICAL RESULTS

Antenna models for both designs are investigated using Finite Element Method (FEM) via Ansys HFSS V.15 simulation tool [34]. Due to the antenna rotational symmetry, incident plane directions are defined in $\varphi = 0^\circ, 30^\circ$ and 45° , and for each of the above defined planes the bistatic radar cross section has been investigated in θ directions as defined in Figure 6.

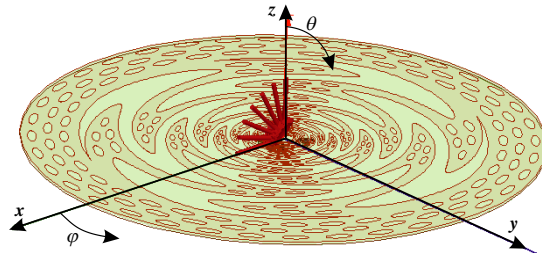


Figure 6. Incident wave direction over the antenna surface for RCS calculation.

To confirm the theoretical expectation on small parasitic openings to the active region current distribution influence, firstly, the antenna analysis is performed, and current distributions are investigated as shown in Figure 7.

The slots openings positions, as defined in Section 2, are chosen to have a minor impact over the edge current distribution as can be seen in Figure 7. From Figure 7, in five slots openings antenna, the current densities present increased maximum values compared to the three slots version. But the difference in the electric potential between the two adjacent sinuous arms remains unchanged. This requirement permits to maintain equivalent magnetic current over the sinuous slots mostly unchanged, and consequently, radiation pattern is remarkably similar in those two antenna models. Parasitic slots dimensions are fraction of the radiation wavelength of the active region of the antenna placed, and

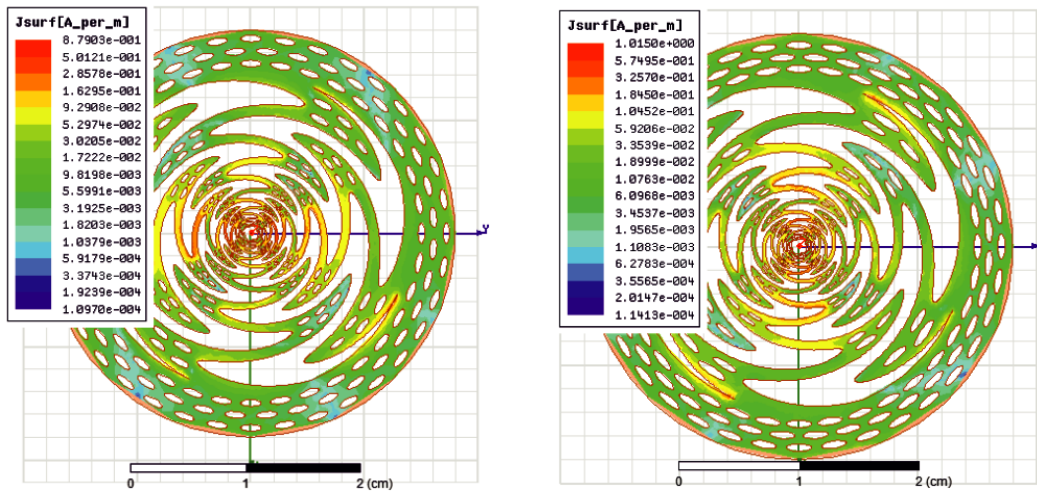


Figure 7. Current density distribution @10 GHz on 5S and 3S antenna models.

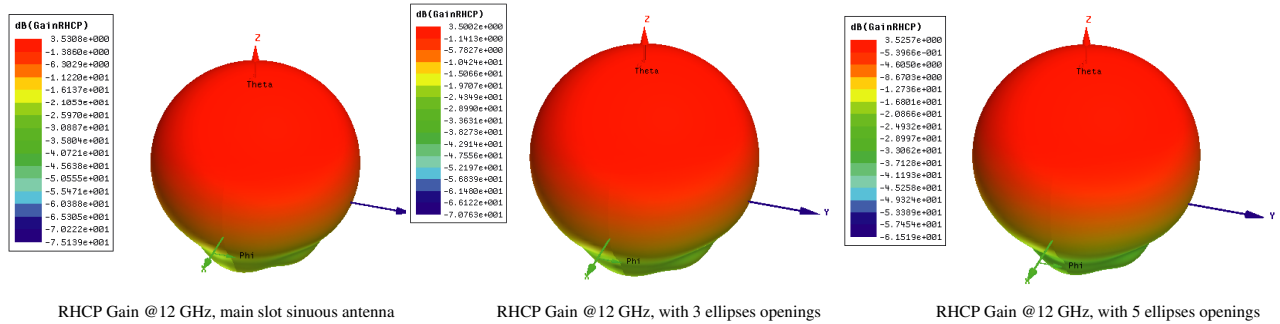


Figure 8. 3D RHCP radiation pattern of the original slot sinuous antenna and the two models proposed.

consequently, their contribution to the radiation field is negligible. This is the motivation on choosing slotted-sinuous antenna version, then the standard sinuous one.

To further confirm this expectations, in Figure 8 for comparison, the 3D radiation patterns of the main slot-sinuous antenna and the two proposed version are presented. As can be evaluated by the relative graphic legend, the maximum gain between those three patterns is approximately of 0.03 dB and can be considered identical for practical point of view.

To better estimate the influence of the ellipses openings to the antenna radiation pattern, Figure 9 present co-polar and cross-polar radiation patterns for all three antenna models on four discrete frequencies in the frequency band.

The radiation pattern is presented for the original slot-sinuous antenna, modified one with 3 ellipses openings antenna, and modified antenna with 5 ellipses openings. Comparing these graphs, we can affirm that the radiation patterns are almost identical and are maintained even when ellipses slots are introduced. The main differences are observed on the cross-polarization pattern, but the results are also comparable.

The focus of this work is to investigate the proposed antenna for bistatic radar cross section and the influence of the proposed ellipses openings on this parameter. Both antenna models are analyzed on the same framework, and the results are presented for bistatic RCS in Figure 10 and Figure 11. Graphics presented in Figure 10 are related to the bistatic structural radar cross section of 3 slots parasitic openings antenna. Presented results are on four relevant frequencies over the entire frequency band and for all the φ analyzed directions planes. The same results are presented in Figure 11 for the 5 slots parasitic openings antenna version.

The two cases are quite similar and are not easy to find differences or to evaluate ellipses openings

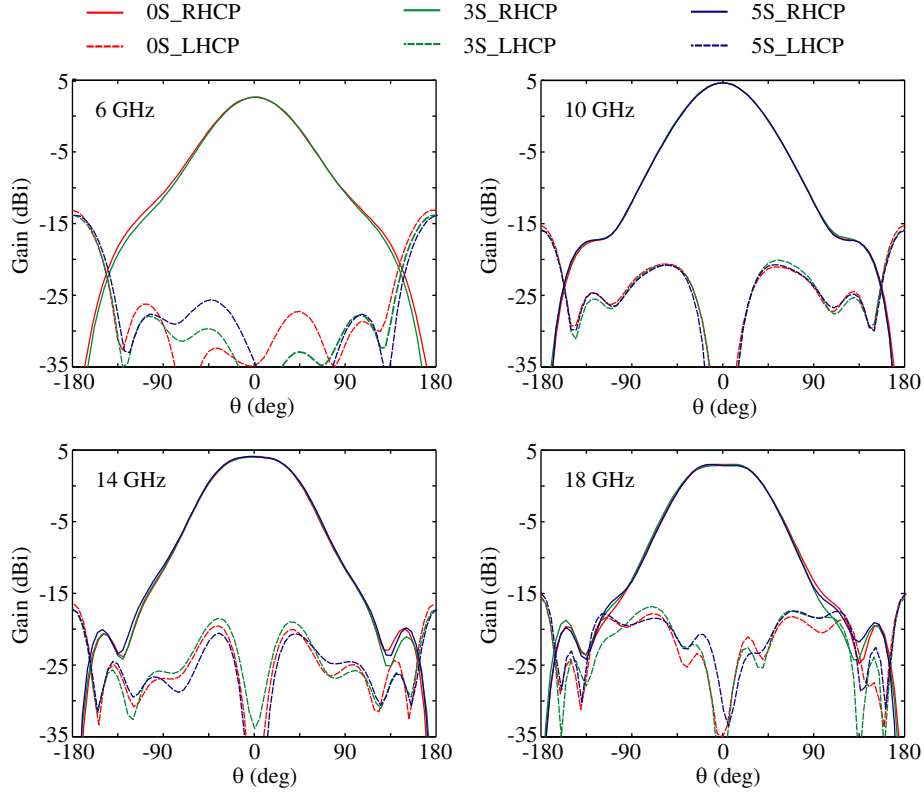


Figure 9. Radiation pattern ($@\phi = 0^\circ$) for main antenna (0S), 3 ellipses openings (3S) and 5 ellipses openings (5S) on four main frequencies on the frequency band.

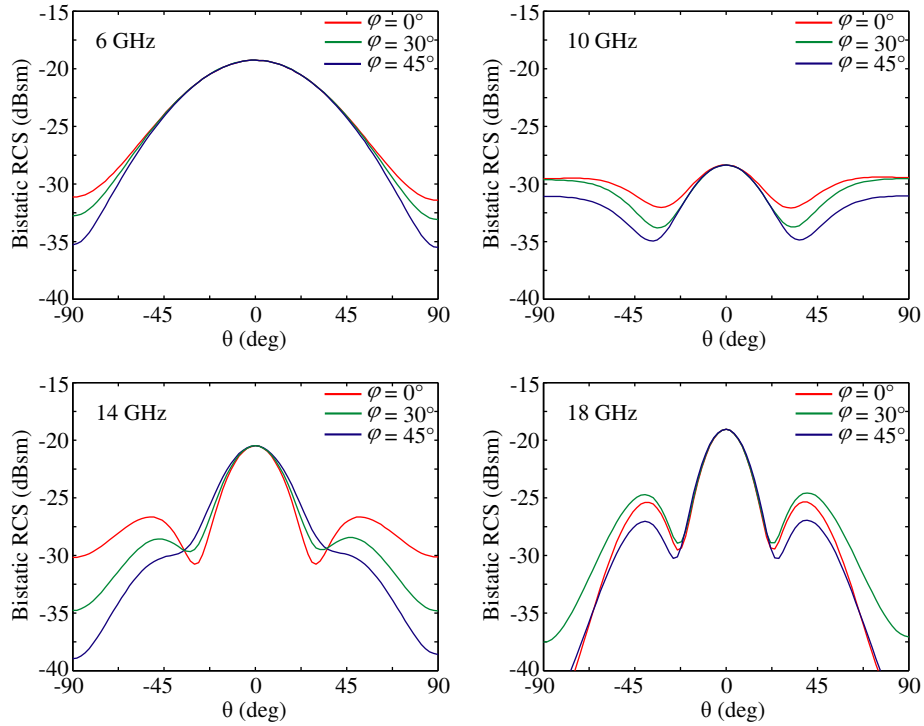


Figure 10. Bistatic Radar Cross Section for different ϕ angles on 3 slot openings antenna.

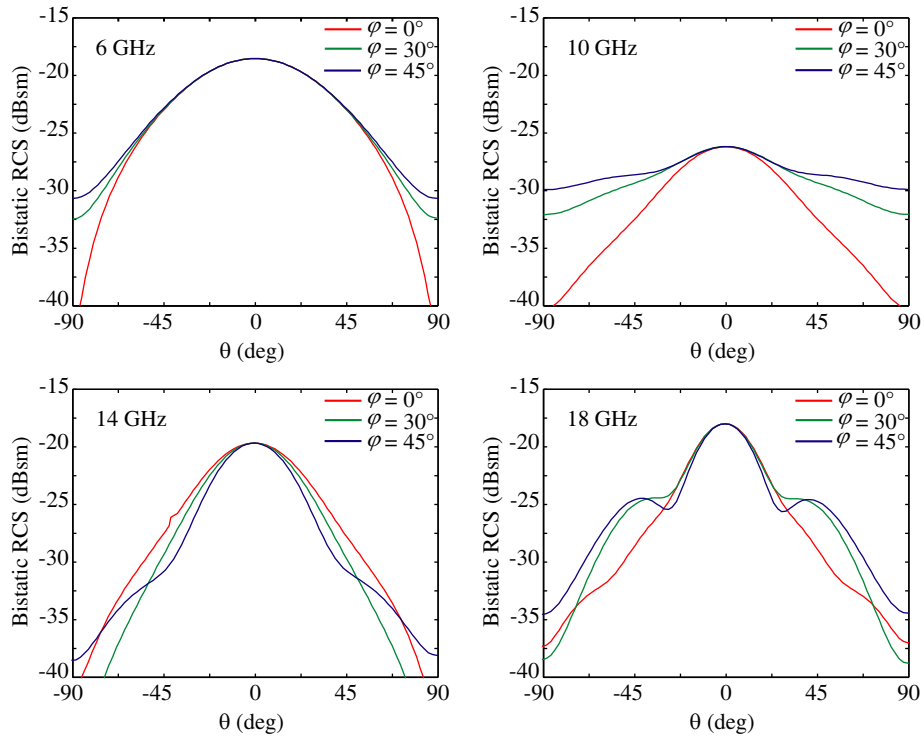


Figure 11. Bistatic Radar Cross Section for different φ angles on 5 slot openings antenna.

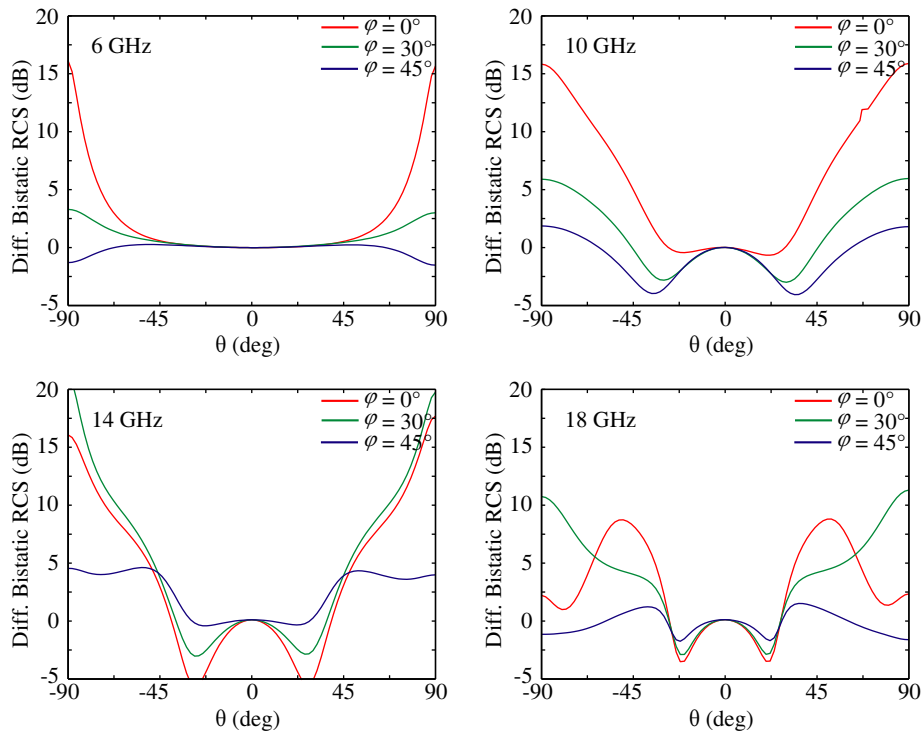


Figure 12. Differences on Bistatic Radar Cross Section for each φ angles for 3 and 5 slot openings antenna.

effect on bistatic RCS. For this purpose, the defined difference in RCS between the two antenna models as in (4) is used to better enhance differences.

Figure 12 presents the bistatic radar cross section differences on the same four relevant frequencies presented in the previous graphics between 3-slot and 5-slot antenna models.

Passing from three slot model to five slot model, a lower bistatic radar cross section is obtained for observation angles directions far from the broadside direction. Referred to Figure 12, for all relevant frequencies, the improvements of bistatic radar cross section up to 15 dB is obtained at 90° from broadside direction. This improvement can be complementary used to antenna shaping which has been conventionally used to reduce monostatic RCS, impacting the bistatic RCS negatively [5].

In observation angles close to the broadside direction, bistatic RCS on 3S model is better than the 5S model. This means that controlling the parasitic openings parameters, an improvement on bistatic RCS can be obtained in the desired bistatic direction.

To better understand the influence of elliptical slots on equivalent radar section, Figure 13 compares the differences ($\Delta\sigma_{3S-0S}$) and the five-slot version with the original antenna ($\Delta\sigma_{5S-0S}$).

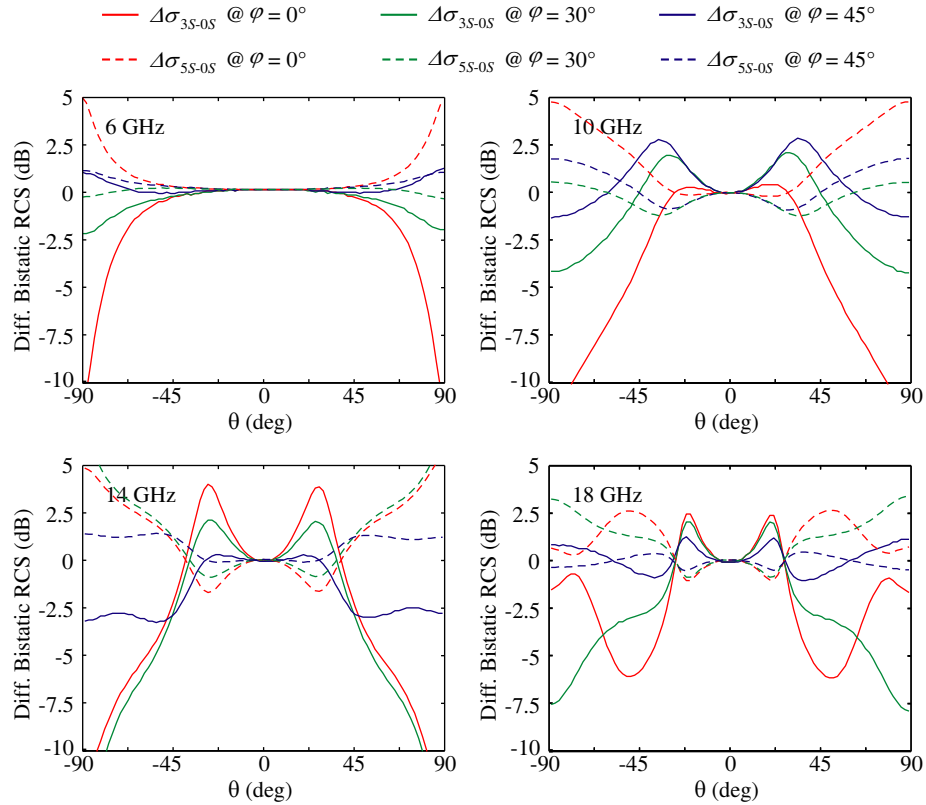


Figure 13. Differences on Bistatic Radar Cross Section for each φ angles for 0, 3 and 5 slot openings antenna.

In the graphs in Figure 13, negative values indicate that the equivalent bistatic radar cross section of the elliptical openings antenna (3S or 5S) is better than the original one without slot (0S), and vice versa. The definition of $\Delta\sigma_{3S-0S} = \sigma_{3Slot} - \sigma_{0Slot}$ and $\Delta\sigma_{5S-0S} = \sigma_{5Slot} - \sigma_{0Slot}$ is as in Equation (4).

It can be understood from these graphs that with the elliptical slots the equivalent bistatic radar cross-section can be controlled. From here, it is understood that by changing the number of openings, their position and size, it is possible to control the equivalent bistatic radar cross-section in the directions of interest, presenting lower or higher values than the antenna without elliptical openings.

In this material, a proof of concept has been proposed and analyzed for bistatic RCS improvements. Changing parasitic slots openings parameters can have a measurable impact on bistatic-RCS in the

desired directions as shown in Figures 10, 11, 12, and 13. The parameters that can allow to control bistatic RCS in the presented slot-sinuuous antenna are five as in the following list:

- N : Total number of ellipses (constrained in the sinuous cell arm);
- A_{max} : Ellipsis major axis dimension (constrained by the available space and total number of ellipses on the cell arm);
- A_R : Ellipsis axial ratio (constrained by the available space in the sinuous cell);
- R : Ellipses radial position from antenna center (constrained in the sinuous cell);
- β : Ellipses position angle (constrained in the sinuous cell);

The overall degree of freedom in designing the presented slot-sinuuous antenna with parasitic ellipses openings is five as above, but their combination results in infinite number of solutions. The ellipses number of each sinuous cell is a discrete number, but all the other variables have infinite combinations. Ellipses axis, radial position, and relative angle position can vary in a continuous solution from a minimal to a maximal dimension based on the relative constraints to maintain the ellipses inside the sinuous cell. Their combination for each discrete number of ellipses for sinuous cell results theoretically in an infinite number of combinations.

Table 2. Comparison of proposed RCS reduction method on UWB antenna with other RCS reduction techniques on existing antennas in literature.

Ref.	Antenna configuration	Modification type	Mono/bi-static	RCS improvement	Frequency band (GHz)
[6]	Double Side Axe Shaped UWB Antenna	Ellipses slot openings to antenna surface and rectangular slots on ground plane	monostatic	up to 15 dB	3.4–15.5
[9]	Rectangular microstrip antenna	Rectangular slots openings to metallic FSS plane	monostatic	up to 12 dB	3–4.86
[12]	Rectangular slot antenna	Polarization conversion metasurface as superstrate	mono/bi-static	up to 10 dB	7.85–12.25
[16]	Circular patch antenna array	EBG based FSS with polarization rotation surface	mono/bi-static	up to 20 dB	6.72–8.25
[21]	1 × 4 microstrip antenna array	Rectangular slots openings on ground plane	monostatic	up to 15 dB	8–12
[22]	Vivaldi antenna	Ellipse slot openings on antenna structure	bistatic	> 19 dB	8–12
[23]	Microstrip antenna	Rectangular slots openings on antenna surface	monostatic	up to 7 dB	3.9–8.1
[24]	Microstrip antenna	Square slots openings on antenna surface	monostatic	up to 7 dB	1–3
[25]	Patch antenna	Cross slots openings on ground plane	monostatic	up to 11 dB	2–20
[30]	Antipodal Vivaldi	Flat corrugated slot line	monostatic	> 3 dB	4.3–12
This work & [19]	Slot-sinuuous antenna	Ellipses slot openings on antenna arms (frequency dependent)	Mono/bi-static	up to 15 dB	6–18

As an example for three slot version, from Table 1, the first ellipse major axis can be set from 0 mm (no ellipse at all) to 35 mm. If we consider a resolution of 100 μm , there are 350 different values just for this parameter. In a similar way, for the other two ellipses, the total combinations of only this parameter are 350^3 , which means 350^3 different antennas to be analyzed. Adding to those parameters, the axial ratio and position, the overall number of different combinations increases rapidly.

In a practical design procedure, the number of all variables is maintained discrete, defined by the physical minimal resolution that can be obtained in the antenna manufacturing process. Even in this case, the total number of combinations is very huge leading to a non-practical designing procedure to analyze all combinations for obtaining the best solution [36].

In conclusion, the number of parameters to be optimized is finite, but their combinations are infinite or very large, and no single optimal solution can be obtained. For a better antenna design with designing goals defined on antenna pattern characteristics, bistatic RCS mask, and manufacturing constraints, a multiobjective optimization technique is suggested to be used [36]. This will be the next evolution of the presented work.

The results presented here for the sinuous antenna and the use of elliptical apertures are in line with what is found in the literature for both monostatic and bistatic radar cross section reduction methods. A partial comparison of the work presented here with similar works in the literature is presented in Table 2.

5. CONCLUSION

The aim of this work is presenting the possibility of controlling bistatic radar cross section of slot-sinuous antenna, by adding parasitic ellipsis openings. Using different parasitic ellipses openings (3 slots, 5 slots or more) not only can be effective in controlling bistatic RCS in endfire direction but also can be used to control in all the other directions.

The number of parasitic openings, their dimensions, and relative position are crucial in obtaining the requested bistatic RCS improvements. Due to the infinite number of parameter combinations, in this work, only two variants are presented as to demonstrate the feasibility of the proposed solution. As a conclusion of the demonstration, it is suggested that the designing process can be carried out with a multi-objective optimization technique where design parameters can be efficiently tuned based on requested RCS and antenna radiation parameters.

This technique can be effectively used for slot-sinuous antenna or similar antennas, where the effective radiations field is obtained by the equivalent magnetic current insured in the slotted version.

REFERENCES

1. Mevoli, G., C. Lamacchia, P. Bia, A. Manna, D. Caratelli, and L. Mescia, "Supershaped sinuous antenna for UWB radar applications," *2021 XXXIVth General Assembly and Scientific Symposium of the International Union of Radio Science (URSI GASS)*, 1–3, IEEE, Aug. 2021, doi: 10.23919/ursigass51995.2021.9560346.
2. Abdollahvand, A., A. Pirhadi, H. Ebrahimian, and M. Abdollahvand, "A compact UWB printed antenna with bandwidth enhancement for in-body microwave imaging applications," *Progress In Electromagnetics Research C*, Vol. 55, 149–157, 2014.
3. Mohanna, M. M., E. A. Abdallah, H. El-Hennawy, and M. A. Attia, "A novel high directive WILLIS-SINHA tapered slot antenna for GPR application in detecting landmine," *Progress In Electromagnetics Research C*, Vol. 80, 181–198, 2018.
4. Hasim, N. S. B., K. A. H. Ping, M. T. Islam, Md. Z. Mahmud, S. Sahrani, D. A. A. Mat, and D. N. A. Zaidel, "A slotted UWB antipodal vivaldi antenna for microwave imaging applications," *Progress In Electromagnetics Research M*, Vol. 80, 35–43, 2019.
5. Alves, M. A., R. J. Port, and M. C. Rezende, "Simulations of the radar cross section of a stealth aircraft," *2007 SBMO/IEEE MTT-S International Microwave and Optoelectronics Conference*, 409–412, 2007, doi: 10.1109/IMOC.2007.4404292.

6. Dikmen, C. M. and G. Çakir, “Double side axe shaped UWB antenna with reduced RCS,” *2013 Asia-Pacific Microwave Conference Proceedings (APMC)*, 215–217, 2013, doi: 10.1109/APMC.2013.6695098.
7. Xu, C., J. Su, and Z. Li, “Radar absorbing material applied to precise RCS regulation of complex scatterer structure,” *2021 IEEE MTT-S International Microwave Workshop Series on Advanced Materials and Processes for RF and THz Applications (IMWS-AMP)*, 388–390, 2021, doi: 10.1109/IMWS-AMP53428.2021.9643935.
8. Pazokian, M., N. Komjani, and M. Karimipour, “Broadband RCS reduction of microstrip antenna using coding frequency selective surface,” *IEEE Antennas and Wireless Propagation Letters*, Vol. 17, No. 8, 1382–1385, Aug. 2018, doi: 10.1109/lawp.2018.2846613.
9. Huang, X., Z. Zhao, and G. Wan, “A slotted frequency selective surface with its application in microstrip antenna RCS reduction,” *2020 IEEE 3rd International Conference on Electronics Technology (ICET)*, 724–728, IEEE, May 2020, doi: 10.1109/icet49382.2020.9119716.
10. Chen, T., Q.-M. Cai, L. Zhu, B.-W. Luo, Y.-Y. Zhu, X. Cao, R. Zhang, N. Feng, and Y.-W. Zhao, “A high-gain, low RCS and dual-frequency microstrip antenna using frequency selective surface,” *2019 Photonics & Electromagnetics Research Symposium — Fall (PIERS — Fall)*, 2249–2254, Xiamen, China, Dec. 17–20, 2019.
11. Zheng, Q., C. Guo, H. Li, and J. Ding, “Broadband radar cross-section reduction using polarization conversion metasurface,” *International Journal of Microwave and Wireless Technologies*, Vol. 10, No. 2, 197–206, Jan. 2018, doi: 10.1017/s1759078717001477.
12. Chatterjee, J., A. Mohan, and V. Dixit, “Radar cross section reduction and gain enhancement of slot antenna using polarization conversion metasurface for X-band applications,” *International Journal of RF and Microwave Computer-Aided Engineering*, Vol. 31, No. 10, e22792, Jul. 2021, doi: 10.1002/mmce.22792.
13. Rajanna, P. K., K. Rudramuni, and K. Kandasamy, “Characteristic mode-based compact circularly polarized metasurface antenna for in-band RCS reduction,” *International Journal of Microwave and Wireless Technologies*, Vol. 12, No. 2, 131–137, Sep. 2019, doi: 10.1017/s1759078719001119.
14. Xie, P., G.-M. Wang, H.-P. Li, Y.-W. Wang, and B. Zong, “Wideband RCS reduction of high gain fabry-perot antenna employing a receiver-transmitter metasurface,” *Progress In Electromagnetics Research*, Vol. 169, 103–115, 2020.
15. Zhu, L., Y. Liu, and Y. Jia, “A broadband low-RCS high-gain circularly polarized holographic antenna based on metasurface,” *2021 International Conference on Microwave and Millimeter Wave Technology (ICMMT)*, 1–2, IEEE, May 2021, doi: 10.1109/icmmt52847.2021.9618044.
16. Parsha, M. K., A. Nandi, and B. Basu, “In-band RCS reduction antennas using an EBG surface,” *International Journal of Microwave and Wireless Technologies*, 1–11, Jun. 2021, doi: 10.1017/s1759078721000933.
17. Modi, A. Y., C. A. Balanis, C. R. Birtcher, and H. N. Shaman, “Novel design of ultrabroadband radar cross section reduction surfaces using artificial magnetic conductors,” *IEEE Transactions on Antennas and Propagation*, Vol. 65, No. 10, 5406–5417, Oct. 2017, doi: 10.1109/tap.2017.2734069.
18. Wang, F., Y. Ren, and K. Li, “Broadband RCS reduction of antenna with AMC using gradually concentric ring arrangement,” *International Journal of Antennas and Propagation*, Vol. 2017, 1–7, 2017, doi: 10.1155/2017/1268947.
19. Agastra, E., A. Biberaj, O. Shurdi, B. Kamo, and A. Rakipi, “RCS analysis on ultra-wideband sinuous antenna with elliptical slots,” *2022 Microwave Mediterranean Symposium (MMS)*, 1–6, IEEE, May 2022, doi: 10.1109/mms55062.2022.9825591.
20. Prasad, B. S. H. and M. V. S. Prasad, “Design and analysis of compact periodic slot multiband antenna with defected ground structure for wireless applications,” *Progress In Electromagnetics Research M*, Vol. 93, 77–87, 2020.
21. Singh, A. and H. Singh, “Low RCS microstrip patch array with hybrid high impedance surface based ground plane,” *Progress In Electromagnetics Research Letters*, Vol. 94, 75–84, 2020.

22. He, X., T. Chen, and X. Wang, "A novel low RCS design method for X-band Vivaldi antenna," *International Journal of Antennas and Propagation*, Vol. 2012, 1–6, 2012, doi: 10.1155/2012/218681.
23. Zhang, J., H. Li, Q. Zheng, J. Ding, and C. Guo, "Wideband radar cross-section reduction of a microstrip antenna using slots," *International Journal of Microwave and Wireless Technologies*, Vol. 10, No. 9, 1042–1047, Aug. 2018, doi: 10.1017/s1759078718000569.
24. Zhang, J., Q. Zheng, H. Li, J. Ding, and C. Guo, "Wideband radar cross section reduction of a microstrip antenna with square slots," *International Journal of Microwave and Wireless Technologies*, Vol. 11, No. 4, 341–350, Feb. 2019, doi: 10.1017/s1759078719000011.
25. Hao, Y., Y. Liu, K. Li, and S. Gong, "Wideband radar cross-section reduction of microstrip patch antenna with split-ring resonators," *Electronics Letters*, Vol. 51, No. 20, 1608–1609, Oct. 2015, doi: 10.1049/el.2015.1725.
26. Mescia, L., G. Mevoli, C. M. Lamacchia, M. Gallo, P. Bia, D. Gaetano, and A. Manna, "Sinuous antenna for uwb radar applications," *Sensors*, Vol. 22, No. 1, 248, 2022, doi: 10.3390/s22010248.
27. Lamacchia, C. M., M. Gallo, L. Mescia, P. Bia, A. Manna, C. Canestri, and D. Gaetano, "Non-conventional cavity backed sinuous antenna for UWB radar applications," *2020 IEEE International Symposium on Antennas and Propagation and North American Radio Science Meeting*, 109–110, IEEE, Jul. 2020, doi: 10.1109/jeeconf35879.2020.9329510.
28. Crocker, D. A. and W. R. Scott, "Sinuous antenna design for UWB radar," *2019 IEEE International Symposium on Antennas and Propagation and USNC-URSI Radio Science Meeting*, 1915–1916, IEEE, Jul. 2019, doi: 10.1109/apusncursinrsm.2019.8888630.
29. Agastra, E., L. Lucci, G. Pelosi, and S. Selleri, "High gain compact strip and slot UWB sinuous antennas," *International Journal of Antennas and Propagation*, Vol. 2012, 1–9, 2012, doi: 10.1155/2012/721412.
30. Luo, T. and Z. Nie, "RCS reduction of antipodal vivaldi antenna," *2015 Asia-Pacific Microwave Conference (APMC)*, Vol. 2, 1–3, IEEE, Dec. 2015, doi: 10.1109/apmc.2015.7413164.
31. Khoomwong, E. and C. Phongcharoenpanich, "Design of ultra-broadband bidirectional ring antenna with superellipse slot using MoM-RWG," *2017 International Symposium on Antennas and Propagation (ISAP)*, 1–2, IEEE, Oct. 2017, doi: 10.1109/isanp.2017.8228998.
32. Bitchikh, M. and F. Ghanem, "A four bandwidth-resolution UWB antipodal vivaldi antenna," *Progress In Electromagnetics Research M*, Vol. 53, 121–129, 2017.
33. Genovesi, S., F. Costa, and A. Monorchio, "Wideband radar cross section reduction of slot antennas arrays," *IEEE Transactions on Antennas and Propagation*, Vol. 62, No. 1, 163–173, Jan. 2014, doi: 10.1109/tap.2013.2287888.
34. ANSYS, "HFSS — High frequency electromagnetic simulation software," <https://www.ansys.com/products/electronics/ansys-hfss>, 2022, accessed: Aug. 12, 2022.
35. Hansen, R., "Relationships between antennas as scatterers and as radiators," *Proceedings of the IEEE*, Vol. 77, No. 5, 659–662, May 1989, doi: 10.1109/5.32056.
36. Agastra, E., G. Pelosi, S. Selleri, and R. Taddei, "Multiobjective optimization techniques," *Wiley Encyclopedia of Electrical and Electronics Engineering*, 1–29, John Wiley & Sons, Inc., Sep. 2014, ISBN 9780471346081, doi: 10.1002/047134608x.w8226.